Contribution from the Department of Chemistry,
University of Iowa, Iowa City, Iowa 52242

Solution Spectroscopic Studies of Electrolytically Generated Iron(III) and Iron(IV) Tetrakis(2,6-difluorophenyl)porphyrin π Cation Radicals

Alaganandan Nanthakumar and Harold M. Goff*

Received September 11, 1990

Electrochemical oxidation of tetrakis(2,6-difluorophenylporphinato)haloiron(III) ([(F8-TPP)Fe^{III}X], where X = Cl^- or F^-) at high potentials in dichloromethane or nitromethane solution results in the generation of iron porphyrin radicals sufficiently stable for spectral characterization at ambient temperature. Proton, deuterium, and fluorine-19 NMR spectroscopic characterization has permitted evaluation of the oxidation state of the metal. Bulk electrolysis at a potential slightly anodic of the first oxidation wave (+1.45 V vs SCE) yields high-spin iron(III) (fluorophenyl)porphyrin radicals that exhibit unique NMR spectral properties in comparison with the nonfluorinated derivatives. Large alternate downfield and upfield phenyl proton and fluorine-19 NMR shifts point to formation of the porphyrin π cation radical with large unpaired spin density at the phenyl ortho fluorine position. Bulk electrolysis of [(F8-TPP)Fe^{III}X] at higher potentials (+1.60 V) results in the generation of an additional product presumably due to the removal of the second electron from the metal center. The NMR spectra of this unstable oxidized product are consistent with an iron(IV) porphyrin π-cation-radical species. Phenyl proton and fluorine signals are drastically shifted in directions opposite to those of the singly oxidized species. Evidence is thus presented for generation of the first iron(IV) porphyrin π-cation-radical species without an axial oxo ligand. Electrochemical oxidation of the dinuclear (μ-oxo)iron(III) porphyrin, [((pyrr-d_8)-F8-TPP)Fe]$_2$O at potentials of +1.20 and +1.50 V yields respective monocation and dication iron(III) porphyrin radical complexes.

Introduction

Oxidation of metalloporphyrins can involve a molecular orbital which is predominantly metal-centered or porphyrin-ring-centered with generation of high-valent iron or porphyrin π-cation-radical species, respectively. Electrochemical oxidation of five-coordinate iron(III) porphyrin halide complexes is known to generate iron(III) π-cation radical species.[1]

High-valent iron porphyrin radical species are proposed as intermediates in the reaction cycles of peroxidases and cytochrome P-450.[2,3] High-valent iron porphyrin radicals having structures analogous to the structure of the compound I intermediate of the peroxidase reaction cycle can be generated by 2-e^- chemical oxidation with oxo-transfer reagents such as *m*-chloroperbenzoic acid at low temperatures.[4,5] Porphyrin phenyl-ring substitution by electron-withdrawing halogens (Cl, F) is known to enhance the stability of high-valent iron porphyrin species.[6,7] The halogenated iron(III) tetraphenylporphyrin complexes reportedly show remarkable resistance toward irreversible oxidative degradation.[8,9] Therefore fluorophenyl-substituted iron(III) porphyrin complexes should provide a rational route for electrochemical generation of kinetically stable radical species at high potentials and also favor metal-centered oxidation. The effect of fluoro substitution on the electronic and spectroscopic properties of these radicals is also of interest.

Previous studies of electrochemically generated radicals of substituted-aryl tetraphenylporphyrins include the low-potential π cation radicals with electron-releasing substituents such as methoxy[1d] and amino groups.[10] This report investigates the solution spectral properties (NMR, UV-visible) of the 1-e^-- and 2-e^--oxidized (F8-TPP)Fe^{III} radical complexes generated by electrochemical methods.

Experimental Section

Iron Porphyrins. Tetraphenylporphyrin ($TPPH_2$) and tetrakis(2,6-difluorophenyl)porphyrin were prepared by the standard pyrrole-arylaldehyde condensation reaction.[11] Deuteriated-pyrrole iron(III) tetraarylporphyrins were prepared by preexchange of pyrrole protons.[12] Iron incorporation was effected by addition of an excess of solid anhydrous $FeCl_2$ to a DMF solution of the porphyrin at reflux under a nitrogen atmosphere.[13] The crude chloroiron(III) tetraphenylporphyrin complex in dichloromethane was purified by passage through a silica gel column. The purified crystalline product was isolated by concentration of the dichloromethane solution with addition of heptane.

The hydroxoiron(III) tetrakis(2,6-difluorophenyl)porphyrin was generated by equilibration of the chloroiron(III) porphyrin complex in dichloromethane with an aqueous sodium hydroxide solution (1 M). The perchloratoiron(III) tetrakis(2,6-difluorophenyl)porphyrin was produced by equilibration of the hydroxoiron(III) porphyrin complex in dichloromethane with aqueous 1 M perchloric acid solution. The dinuclear (μ-oxo)iron(III) complex, [(F8-TPP)Fe]$_2$O, was produced by equilibration of the perchloratoiron(III) tetrakis(2,6-difluorophenyl)porphyrin complex in dichloromethane with distilled water. The fluoroiron(III) porphyrin complex was generated by equilibration of the dichloromethane solution of the chloroiron(III) porphyrin complex with aqueous 1 M HF solution. The crystalline products were isolated by concentration of the respective dichloromethane solution with addition of heptane. The products were characterized by proton and fluorine NMR and UV-visible spectroscopic measurements.

Electrochemical Techniques. Tetraalkylammonium salts utilized as supporting electrolytes were purified by recrystallization from 1:4 acetonitrile/water and dried under vacuum. Electrochemical bulk oxidations were performed with a three-electrode cell configuration that employed a Princeton Applied Research (PAR) Model 173 potentiostat. Supporting electrolyte concentrations were 0.1 M, and iron porphyrin concentrations were 2.0-5.0 mM. The reference electrode consisted of a silver wire immersed in a 0.1 M $AgNO_3$/acetonitrile solution separated from the bulk solution by porous Vycor glass. The counter electrode was a platinum coil immersed in 0.1 M supporting electrolyte solution in a separate glass tube fitted with a very fine glass frit. A cylindrical platinum gauze was used as the working electrode. In a typical electrolysis experiment 2.0-5.0 mM iron porphyrin dissolved in 5-10 mL of solvent was electrolyzed at a potential anodic (10-20 mV) of the voltammetric peak potential. The electrolysis was stopped when the current had

(1) (a) Phillippi, M. A.; Shimomura, E. T.; Goff, H. M. *Inorg. Chem.* **1981**, *20*, 1322-1325. (b) Gans, P.; Marchon, J.-C.; Reed, C. A.; Regnard, J.-R. *Nouv. J. Chim.* **1981**, 203-204. (c) Shimomura, E. T.; Phillippi, M. A.; Goff, H. M.; Scholz, W. F.; Reed, C. A. *J. Am. Chem. Soc.* **1981**, *103*, 6778-6780. (d) Phillippi, M. A.; Goff, H. M. *J. Am. Chem. Soc.* **1982**, *104*, 6026-6034. (e) Scholz, W. F.; Reed, C. A.; Lee, Y. J.; Scheidt, W. R.; Lang, G. *J. Am. Chem. Soc.* **1982**, *104*, 6791-6793. (f) Gans, P.; Buisson, G.; Duee, E.; Marchon, J.-C.; Erler, B. S.; Scholz, W. F.; Reed, C. A. *J. Am. Chem. Soc.* **1986**, *108*, 1223-1234.
(2) (a) Dunford, H. B.; Stillman, J. S. *Coord. Chem. Rev.* **1976**, *19*, 187-251. (b) Dunford, H. B. *Adv. Inorg. Biochem.* **1982**, *4*, 41-68.
(3) Groves, J. T. In *Cytochrome P-450: Structure, Mechanism and Biochemistry*; Ortiz de Montellano, P., Ed.; Plenum Press: New York, 1985; Chapter I and references therein.
(4) (a) Groves, J. T.; Haushalter, R. C.; Nakamura, M.; Nemo, T. E.; Evans, B. J. *J. Am. Chem. Soc.* **1981**, *103*, 2884-2886. (b) Boso, B.; Lang, G.; McMurry, T. J.; Groves, J. T. *J. Chem. Phys.* **1983**, *79*, 1122-1126.
(5) Hickman, D. L.; Nanthakumar, A.; Goff, H. M. *J. Am. Chem. Soc.* **1988**, *110*, 6384-6390.
(6) Gold, A.; Jeyaraj, K.; Doppelt, P.; Weiss, R.; Chottard, G.; Bill, E.; Ding, X.; Trautwein, A. X. *J. Am. Chem. Soc.* **1988**, *110*, 5756-5761.
(7) Nanthakumar, A.; Goff, H. M. *J. Am. Chem. Soc.* **1990**, *112*, 4047-4049.
(8) Chang, C. K.; Ebina, F. *J. Chem. Soc., Chem. Commun.* **1981**, 778.
(9) Traylor, P. S.; Dolphin, D.; Traylor, T. G. *J. Chem. Soc., Chem. Commun.* **1984**, 279.
(10) Chang, D.; Cocolios, P.; Wu, Y. T.; Kadish, K. M. *Inorg. Chem.* **1984**, *23*, 1629-1633.
(11) Fuhrhop, J.-H.; Smith, K. M. In *Porphyrins and Metalloporphyrins*; Smith, K. M., Ed.; Elsevier: New York, 1975; pp 769-770.
(12) Shirazi, A.; Goff, H. M. *J. Am. Chem. Soc.* **1982**, *104*, 6318-6322.
(13) (a) Adler, A. D.; Longo, F. R.; Kampus, F.; Kim, J. *J. Inorg. Nucl. Chem.* **1970**, *32*, 2443-2445. (b) Adler, A. D.; Longo, F. R.; Varadi, V. *Inorg. Synth.* **1976**, *16*, 213-220.

0020-1669/91/1330-4460$02.50/0

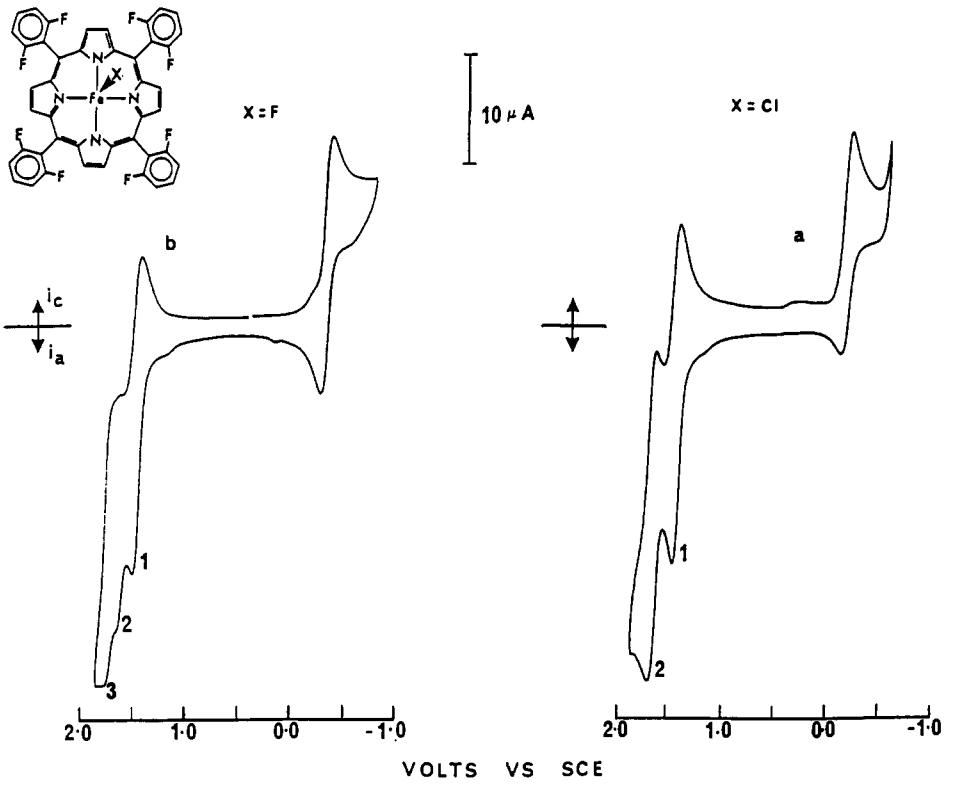

Figure 1. Cyclic voltammetric traces of (F8-TPP)$Fe^{III}X$ in dichloromethane (0.1 M Pr_4NClO_4, 2 mM iron porphyrin, 25 °C, potentials adjusted to the SCE reference): (a) X = Cl^-; (b) X = F^-. Scan rate = 50 mV/s.

dropped to 10–20% of the initial value. Typical electrolysis times ranged from 60 to 90 min, depending on the concentration of iron porphyrin. Small aliquots of electrolysis solution were transferred to NMR tubes or UV-visible cells for analyses. Mixing of the solution was ensured by continuous bubling with solvent-saturated nitrogen gas, which also maintained an inert atmosphere. A PAR Model 175 universal programmer along with the PAR Model 173 potentiostat was used for cyclic voltammetric measurements. A platinum-bead working electrode was used for voltammetric measurements. Potentials were adjusted to the conventional aqueous SCE reference by application of a factor of 0.38 V. This conversion factor was calculated as previously described.[5] The ferrocenium/ferrocene potential ($E_{1/2} = (E_{p,a} + E_{p,c})/2$) was +0.15 V in CH_2Cl_2 with the Ag/Ag^+ (0.1 M)–CH_3CN reference and a Pt working electrode.

Instrumental Techniques. Proton and deuterium NMR measurements were carried out at 360 and 55 MHz, respectively, on a Bruker WM-360 pulsed FT spectrometer or at 300 and 46 MHz, respectively, on a Bruker MSL-300 pulsed FT instrument. ^{19}F NMR spectroscopy was carried out on the Bruker MSL-300 spectrometer at 282 MHz. UV–visible measurements were performed with a HP 8452A diode array spectrophotometer.

Results

Cyclic Voltammetric Studies. Figure 1 illustrates the voltammetric behavior of (F8-TPP)$Fe^{III}X$ complexes (X = Cl^-, F^-). The potentials for the first oxidation waves are identical for the fluoro, chloro, and perchlorato complexes (at +1.45 V vs SCE), which is an indication that the electron removal occurs from a porphyrin-ligand-centered molecular orbital. The Fe(III)/Fe(II) reduction potentials correlate with the axial ligand strength ($E°$ = +0.25, −0.15, −0.35, and −0.70 V for X = ClO_4^-, Cl^-, F^-, and OH^-, respectively). The chloroiron(III) porphyrin complex shows two well-defined oxidation waves whereas the fluoro complex shows considerable overlap between the first and second oxidation waves (waves 1 and 2 of Figure 1a,b). The sensitivity of the second oxidation wave to axial ligand field strength is an indication that this oxidation is due to the removal of an electron from a metal-centered molecular orbital. Similar voltammetric behavior is observed in nitromethane solvent. The peak to peak separation of the anodic and cathodic waves of 70–80 mV is consistent with 1-e^- oxidation for both waves 1 and 2. The resistive nature of dichloromethane solvent makes this value higher than the expected 59-mV peak separation. The perchlorato complex shows only one reversible oxidation wave at +1.45 V (not shown). The absence of a second oxidation wave at higher potentials for this complex is probably due to degradation of the porphyrin ligand.

The voltammetric behavior for the hydroxoiron(III) porphyrin complex shows an irreversible oxidation wave at a potential (+1.40 V vs SCE) slightly cathodic of the potential for the first oxidation wave of the fluoro, chloro, and perchlorato complexes. The reduction wave corresponding to this oxidation is not observed even at higher potential scan rates (200 mV/s) or upon reversal of the potential sweep at more cathodic potentials. The highly reactive nature of this oxidized product is thus indicated. The irreversible oxidation wave is probably due to the initial generation of an unstable high-valent iron porphyrin species and parallels results of other types of hydroxoiron(III) porphyrin complexes.[14] The irreversible wave is followed by a reversible oxidation wave at a potential consistent with removal of an electron from the porphyrin ring (+1.45 V vs SCE).

The cyclic voltammetric trace for [(F8-TPP)Fe]$_2$O shows two reversible waves at $E°$ = 1.10 and 1.40 V (vs SCE), which correspond to the removal of an electron from each porphyrin ring, respectively. The positive shift in redox potential relative to the unsubstituted porphyrin dimer (first oxidation peak potential for [(TPP)Fe]$_2$O is at +0.85 V) is expected due to the electron-withdrawing *o*-fluorophenyl substituent. A third, irreversible oxidation wave is also observed at $E_{p,a}$ = 1.70 V and is associated with cleavage of the dimer to generate a monomeric species.

NMR Studies of Electrochemically Oxidized (F8-TPP)$Fe^{III}X$. Figure 2 shows the deuterium NMR spectra of the products formed following bulk electrolysis of ((pyrr-d_8)-F8-TPP)$Fe^{III}Cl$ in dichloromethane with Pr_4NClO_4 supporting electrolyte at potentials anodic of the first and second oxidation waves (waves 1 and 2 of Figure 1a). Deuteriated porphyrins are well suited for NMR studies of bulk electrolytic products, as the signals due to the large excess of tetraalkylammonium salts present as sup-

(14) (a) Lee, W. A.; Calderwood, T. S.; Bruice, T. C. *Proc. Natl. Acad. Sci. U.S.A.* **1985**, *82*, 4301–4305. (b) Swistak, C.; Mu, X. H.; Kadish, K. M. *Inorg. Chem.* **1987**, *26*, 4360–4366.

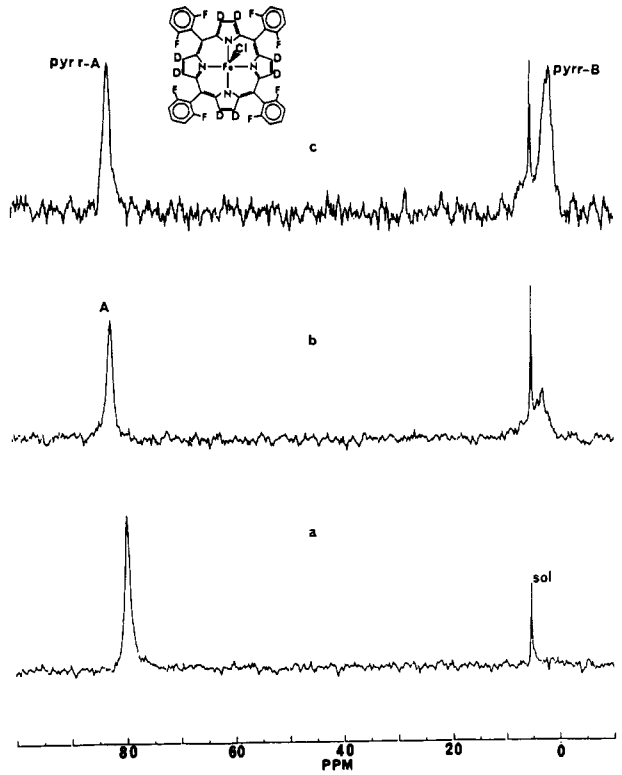

Figure 2. Deuterium NMR (46 MHz) spectra of the products generated after oxidative bulk electrolysis of ((pyrr-d_8)-F8-TPP)$Fe^{III}Cl$ in dichloromethane (0.1 M Pr_4NClO_4, 2 mM iron porphyrin, 25 °C): (a) before electrolysis; (b) after electrolysis at +1.48 V; (c) after electrolysis at +1.65 V. Potentials are referenced with respect to the SCE.

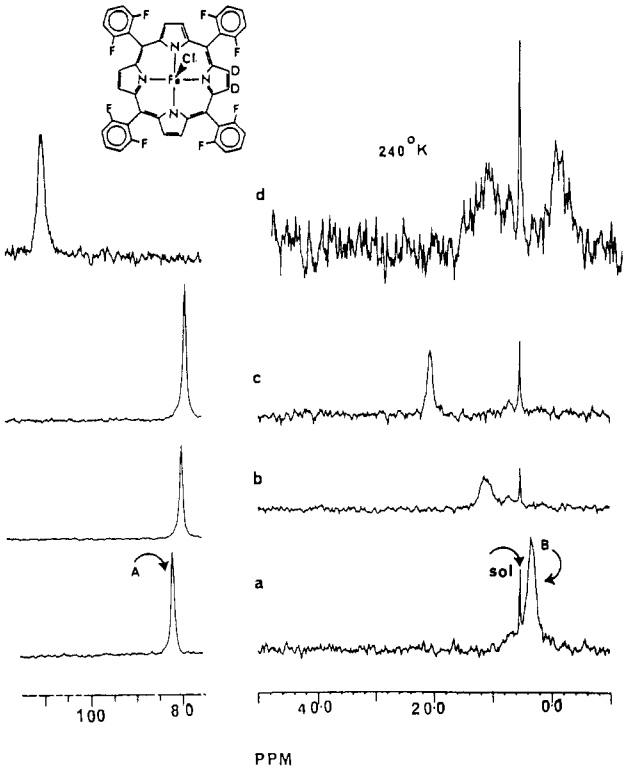

Figure 3. Effect of reduction and temperature change on deuterium NMR (55 MHz) spectra of the products generated after bulk electrolysis of ((pyrr-d_8)-F8-TPP)$Fe^{III}Cl$ at +1.60 V (vs SCE) in dichloromethane (0.1 M Pr_4NClO_4, 5 mM iron porphyrin): (a) spectrum immediately after electrolysis at 25 °C; (b) spectrum after titration of solution a with approximately 0.75 equiv of (F8-TPP)$Fe^{III}Cl$ at 25 °C; (c) spectrum after titration with excess (2.5 equiv) (F8-TPP)$Fe^{III}Cl$; (d) spectrum of solution a at 240 K.

porting electrolyte are of minimal intensity (from natural-abundance deuterium). The position of the pyrrole chemical shift also gives information about the oxidation and spin states of iron porphyrins (vide infra).

Oxidation at a potential anodic of wave 1 (+1.48 V vs SCE) results in a downfield shift of the pyrrole deuteron signal from 79.8 ppm for the parent complex (Figure 2a) to 82.5 ppm for the oxidized product (signal A, Figure 2b). Increasing the applied potential to +1.65 V results in the generation of an additional product (signal B, Figure 2c) at +2.0 ppm and a further downfield-shifted signal A (84.0 ppm). The chemical shifts and relative areas of both signals depend on the applied potential, time of electrolysis, and initial concentration of (F8-TPP)$Fe^{III}Cl$. This implies that signals A and B represent mixtures of complexes, part of which are in rapid electron exchange on the 55-MHz time scale. Signal A moves in an upfield direction toward the pyrrole signal position for (F8-TPP)$Fe^{III}Cl$, and signal B moves in a downfield direction with time. These observations indicate that signals A and B are due to products associated with electron removal corresponding to oxidative waves 1 and 2 (Figure 1a), respectively. The variable chemical shift of signal A is due to a mole fraction weighted average between the parent and singly oxidized complexes. Complete electrolysis to generate the oxidized products exclusively was not possible due to competing autoreduction of the reactive species. The maximum shifts observed in dichloromethane solution for signals A and B were 85.0 and 0.5 ppm, respectively, using a relatively low concentration of (F8-TPP)-$Fe^{III}Cl$ (1.5 mM) with electrolysis at a potential of 1.67 V.

The solution composition that gives rise to signals A and B in Figure 2 is clarified by addition of parent (F8-TPP)$Fe^{III}Cl$ and by variable-temperature measurements. Figure 3a shows the deuterium NMR spectrum obtained after bulk electrolysis of ((pyrr-d_8)-F8-TPP)$Fe^{III}Cl$ at +1.60 V in dichloromethane. The chemical shifts of signals A and B are 82.5 and 3.5 ppm, respectively. Addition of 0.75 equiv of nondeuteriated (F8-TPP)-$Fe^{III}Cl$ results in the movement of signal B to lower field with diminished intensity and area (Figure 3b). Signal A correspondingly moves in an upfield direction. Addition of excess (F8-TPP)$Fe^{III}Cl$ results in the movement of signal B to 20.5 ppm (Figure 3c), which is in the region observed for the perchloratoiron(III) porphyrin species in CH_2Cl_2. Signal A correspondingly moves to 79.8 ppm with an enhancement of area. In order to slow the rate of electron and/or ligand exchange, the freshly electrolyzed solution was cooled (240 K), and as expected, signal B split into two peaks (Figure 3d) corresponding to the perchloratoiron(III) species (10 ppm) and the high-potential product (−2 ppm). The peaks merged upon return to ambient temperature. A rapid electron-transfer rate was evident even at 210 K for species associated with signal A and the parent (F8-TPP)$Fe^{III}Cl$ (on the 55-MHz NMR time scale), as no splitting was observed for the corresponding peak (Figure 3d).

Similar results are also observed for the (F8-TPP)$Fe^{III}F$ complex with bulk oxidation at the second wave. However, the intensity of the NMR signal for the oxidized product corresponding to signal B was relatively weak. This may be due to a third oxidation process (wave 3, Figure 1b), which overlaps with the oxidation peak potential for wave 2 of Figure 1b. Bulk oxidation of (F8-TPP)$Fe^{III}ClO_4$ at potentials higher than +1.45 V resulted in precipitation of insoluble degradation products. This result rules out the possibility that the species associated with signal B is a five-coordinate perchloratoiron(III) porphyrin radical.

Chemical shift data for the phenyl protons also give valuable information with regard to the radical unpaired spin distribution in the tetraarylporphyrin ring and the oxidation state of the metal.[1d,5] Table I lists the limiting chemical shift values for the phenyl proton and fluorine NMR signals for species corresponding to signals A and B of Figures 2 and 3. Nitromethane-d_3 was used as the electrolytic solvent for proton NMR analysis. As a high dielectric, less volatile, relatively low cost deuteriated solvent and a radical-trapping agent, nitromethane has advantages over dichloromethane. Accordingly, the radical species were relatively more stable and hence showed larger limiting chemical shift values

Table I. NMR Chemical Shift Values for Iron(III) Porphyrins and Oxidized Products (25 °C; Proton Signals Referenced to $(CH_3)_4Si$; ^{19}F Signals Referenced to $CFCl_3$)

	(F8-TPP)$Fe^{III}Cl$[a]	species A[b] (−1 e⁻)	species B[b] (−2 e⁻)	(TPP)$Fe^{III}Cl^{+}$[c]
ortho H				37.6
ortho F	−78.5, −81.0	−140	10	
meta H	13.5, 11.8	−3.5, −4.5	30.5	−12.4
para H	7.0	16.0	−2.0	29.5
pyrr H (or ^2H)	80.0	85.5	−5.0	65.0

[a] CD_2Cl_2 solvent. [b] Proton spectrum recorded in CD_3NO_2; ^{19}F spectrum recorded in CH_2Cl_2; chemical shift values approximate due to competing autoreduction. [c] Singly oxidized (TPP)$Fe^{III}Cl$ product.[1d]

compared with dichloromethane solvent. Phenyl proton signals were readily assigned on the basis of area ratios (meta H:para H = 2:1) for CD_3NO_2 solutions electrolyzed at potentials of +1.45 and +1.60 V. As was observed for the pyrrole deuteron signals, the proton and fluorine NMR signals of the oxidized products slowly (2–3 h) moved toward the chemical shift values of the parent (F8-TPP)$Fe^{III}Cl$ complex. Hence, the observed phenyl signals are also a representation of the mole fraction weighted average shift of the oxidized and unoxidized complexes.

The ^{19}F NMR chemical shift data are also included in Table I for the parent (F8-TPP)$Fe^{III}Cl$ and for the singly and doubly oxidized compounds. The *o*-fluorophenyl doublet observed for the unoxidized complex at −78.5 and −81.0 ppm (vs $CFCl_3$) was converted to a broad, upfield-shifted signal with progressive oxidation at potentials up to +1.60 V. The apparent limiting ^{19}F chemical shift value for the singly oxidized complex in dichloromethane solution was seen at −140 ppm. Bulk electrolysis at +1.65 V was associated with the appearance of a new ^{19}F signal shifted drastically in the downfield direction to at least +10 ppm. The position and intensity of this signal were dependent on the applied potential and electrolysis time, much as was the case for the pyrrole deuteron signal "B" for the doubly oxidized product in Figure 1.

NMR Study of [(F8-TPP)Fe^{III}]$_2$O Oxidation. Proton NMR spectra have been reported for singly and doubly oxidized (TPP)$Fe^{III}]_2O$.[1d,15] The pyrrole proton chemical shifts (10–13 ppm) are much smaller than for the five-coordinate high spin (TPP)Fe^{III} complexes as a result of antiferromagnetic coupling through the oxo bridge. The pyrrole deuteron NMR signals for the products prepared by bulk electrolysis of [((pyrr-d_8)-F8-TPP)Fe]$_2$O at potentials slightly anodic of the first (+1.20 V) and the second (+1.50 V) voltammetric waves are observed at +4.5 and −4.0 ppm, respectively (Figure 4b,c). These represent the chemical shifts for the fully delocalized mono- and dications, respectively.

The dication species is stable in the electrolytic solution (1–2 h) at ambient temperature. The dication is converted to a mixture of [(F8-TPP)Fe]$_2O^+$ and [(F8-TPP)Fe]$_2$O by addition of excess [(F8-TPP)Fe]$_2$O parent complex (Figure 4d). This observation confirms the retention of the oxidized dimeric structure in solution. The porphyrin pyrrole signal for the monocation moves in the downfield direction with autoreduction, and examination after 24 h (Figure 4e) revealed the pyrrole deuteron signal for the parent [(F8-TPP)Fe]$_2$O. Therefore, the observed shift represents a mole fraction weighted average due to rapid electron transfer on the 55-MHz NMR time scale between the oxidized and parent complexes.

A relatively large shift is also observed for the *o*-fluorophenyl NMR signals of [(F8-TPP)Fe]$_2$O upon oxidation. The fluorine NMR spectrum of [(F8-TPP)Fe]$_2$O shows two signals at −102.8 and −109.2 ppm (Figure 5a). The ^{19}F NMR spectrum obtained after bulk electrolysis at +1.20 V to generate the monocation has the *o*-fluorophenyl signals at −73.5 and −94.0 ppm (Figure 5b; secondary products are also identified). The ^{19}F NMR spectrum of the dication generated by bulk electrolysis at +1.40 V shows two signals at −66.0 and −91.0 ppm, which represent an *o*-fluorophenyl splitting of 25.0 ppm (Figure 5c). However, in

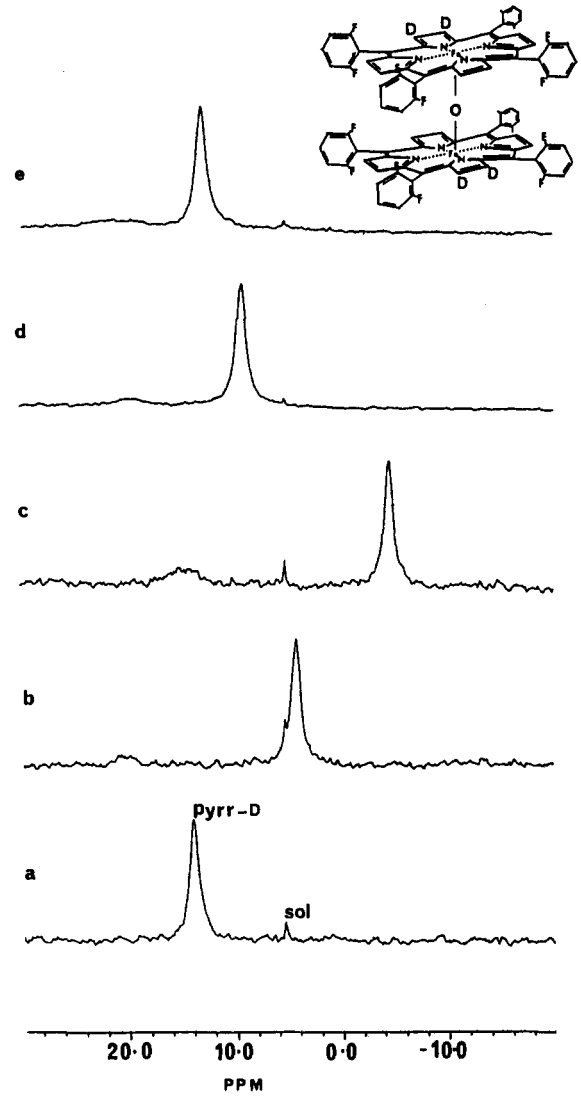

Figure 4. Deuterium NMR spectra (55 MHz) of the bulk electrolytic products of [((pyrr-d_8)-F8-TPP)$Fe^{III}]_2O$ (2 mM; dichloromethane solvent, 0.1 M Pr_4NClO_4, 25 °C): (a) Spectrum recorded before electrolysis; (b) spectrum after electrolysis at +1.20 V (vs SCE); (c) spectrum after electrolysis at +1.40 V; (d) spectrum immediately after addition of excess [((pyrr-d_8)-F8-TPP)$Fe^{III}]_2O$ to solution c; (e) spectrum of solution d after 24 h at room temperature.

comparison with those of the monocation, the *o*-fluorophenyl line widths of the dication are considerably narrowed, presumably due to efficient electron spin–spin relaxation within the diradical complex.

Electronic Spectroscopic Studies. Electronic spectra of the singly oxidized (F8-TPP)$Fe^{III}Cl$ derivative reveal a blue-shifted Soret band with diminished intensity at 382 nm, as compared with a Soret band for the parent iron(III) porphyrin at 406 nm. Weak bands at 630 and 690 nm are also seen in the optical spectrum of the singly oxidized product. Blue-shifted Soret bands of diminished intensity are a general feature of the electronic spectra of iron(III) and iron(IV) porphyrin π cation radicals,[16-18] and hence these spectra are fully consistent with the interpretation of NMR data. After a period of 24 h, the singly oxidized product was autoreduced to the parent (F8-TPP)$Fe^{III}Cl$ complex, as judged by the electronic spectrum. Competitive autoreduction precluded generation of the doubly oxidized product as a predominant

(15) Phillippi, M. A.; Goff, H. M. *J. Am. Chem. Soc.* **1979**, *101*, 7641–7643.

(16) Felton, R. H.; Owen, G. S.; Dolphin, D.; Fajer, J. *J. Am. Chem. Soc.* **1971**, *93*, 6332–6334.

(17) Felton, R. H.; Owen, G. S.; Dolphin, D.; Forman, A.; Borg, D. C.; Fajer, J. *Ann. N.Y. Acad. Sci.* **1973**, *206*, 504–514.

(18) Calderwood, T. S.; Lee, W. A.; Bruice, T. C. *J. Am. Chem. Soc.* **1985**, *107*, 8272–8273.

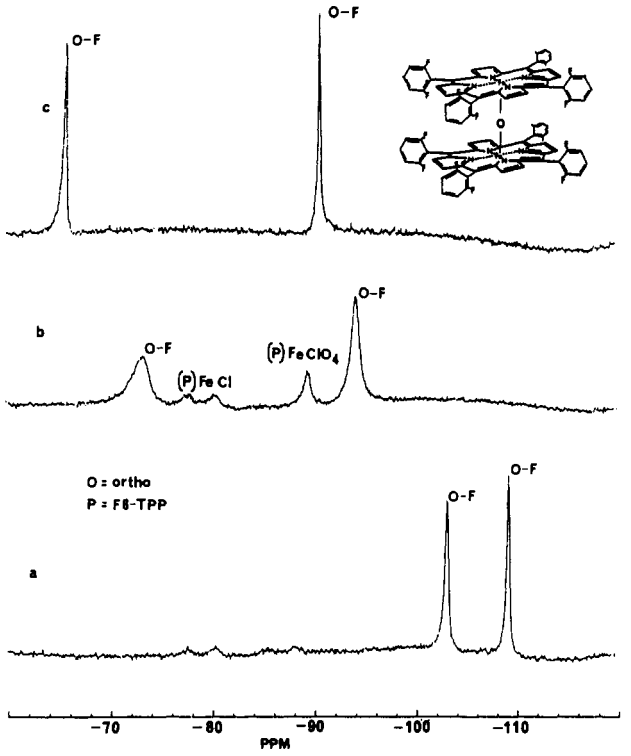

Figure 5. Fluorine NMR (290 MHz) spectra of the bulk electrolytic products of $[(F8\text{-}TPP)Fe^{III}]_2O$ in dichloromethane solvent (0.1 M Pr_4NClO_4, 25 °C, 2 mM iron porphyrin dimer): (a) before electrolysis; (b) after electrolysis at +1.20 V; (c) after electrolysis at +1.40 V. All potentials are referenced with respect to the SCE. Chemical shifts are referenced with respect to $CFCl_3$.

product for electronic spectroscopy.

Discussion

Two types of π cation radicals have been reported for metalloporphyrins.[19-22] Large spin density at the bridging meso-carbon atom and at the pyrrole nitrogen atom is characteristic for the a_{2u} radicals. A relatively small change in the pyrrole proton isotropic shift upon oxidation is generally indicative of an a_{2u} radical type, given negligible radical spin density at this position. Through a spin-polarization mechanism the spin density at the meso-carbon atom is transferred to the phenyl group. Hence, alternate upfield and downfield proton NMR signals are observed for the phenyl ortho, meta, and para protons of iron(III) tetraphenylporphyrin π cation radicals.[1d] At the other extreme, the a_{1u} radical has spin density concentrated at the pyrrole carbon atom. Hence, a large change in the isotropic shift of the pyrrole proton NMR signal is expected for generation of this radical type.

The alternate upfield and downfield signals for the phenyl meta and para protons of singly and doubly oxidized (F8-TPP)FeCl are similar to those observed for unsubstituted iron(III) tetraarylporphyrin radicals. However, the magnitudes of phenyl proton chemical shifts are comparatively smaller, as may be seen in Table I. The small shift of the pyrrole proton (or deuteron) signal upon oxidation (from 80.0 to 85.5 ppm in nitromethane) is indicative of negligible unpaired spin density being placed on the pyrrole β-carbon atom, as expected for a_{2u} type radicals. The small downfield pyrrole proton shift upon oxidation is to be contrasted with a somewhat larger upfield shift to 65 ppm for the unsubstituted chloroiron(III) tetraphenylporphyrin radical. The basis for this difference between porphyrins is not clear, but could be a consequence of changes in spin–spin coupling of iron(III) and radical spins or rearrangement of spin density on the porphyrin ring induced by inductive and resonance effects of the *o*-fluorophenyl substituents.

The direction of the phenyl meta and para proton and fluorine NMR chemical shifts are reversed for the doubly oxidized product ("B") when compared with the singly oxidized product ("A"). This may result from a change in either the oxidation state or the spin state of the metal. Ample precedent exists for change in direction of phenyl signals for porphyrin radical complexes of iron(III) in various spin and oxidation states.[1d,15,23] The phenyl meta and para proton shift directions are common to those reported for a putative fluorooxoiron(IV) tetraphenylporphyrin π cation radical. The pyrrole deuteron chemical shift of +0.5 ppm observed for the doubly oxidized product in CH_2Cl_2 is in the region observed for oxoiron(IV) porphyrins and oxoiron(IV) porphyrin π-cation-radical species.[5] There is, however, no indication that product B (Figure 2) bears an oxo ligand, and the solution characterization of species B provides evidence for generation of an iron(IV) porphyrin π cation radical with chloro and likely perchlorato axial ligation. Hence, *o*-fluorophenyl substitution perturbs the porphyrin electronic structure such that the second oxidation potential of the ring is higher than that for metal oxidation, even though the metal ion does not contain a highly basic ligand.

Large ^{19}F chemical shifts for fluorophenyl groups of the iron porphyrin radical species merit comment. The change in *o*-fluorophenyl ^{19}F chemical shift from approximately −80 to −140 ppm upon oxidation of $(F8\text{-}TPP)Fe^{III}Cl$ is to be compared with a phenyl ortho proton chemical shift change from 6 to 37.6 ppm for oxidation of $(TPP)Fe^{III}Cl$. Fluorine and proton shifts are opposite in direction, and the radical-induced ^{19}F shift is approximately twice as large. This pattern quantitatively replicates that seen in other partially fluorinated aromatic radicals in that the radical-induced ^{19}F shift is 2-fold greater than and opposite in sign to that for the respective proton.[24] This is apparently due to a balance of spin polarization from the attached carbon and from the 2p orbital of the fluorine atom.[24]

No simple explanation can be offered for the upfield shift of the pyrrole deuteron signal associated with single and double oxidation of $[(F8\text{-}TPP)Fe]_2O$. Although the pyrrole deuteron signal detected at −4.0 ppm for the doubly oxidized product of $[(F8\text{-}TPP)Fe]_2O$ is in the region typical for iron(IV) porphyrin species,[4,5] the large shifts observed for the *o*-fluorophenyl NMR signals (Figure 5) of the oxidized products are indicative of radical species. Hence, the oxo-bridged dinuclear compounds are best described as mono- and dication radicals.

It is noteworthy that the *o*-fluorophenyl substituents should have such a dramatic effect on the redox potentials and rearrangement of spin density in the iron porphyrin π cation radicals. The generality of the a_{2u} radical formalism is brought into question for tetraarylporphyrins with diverse substituents. Alternately, the fluorophenyl derivatives may have anomalous electronic properties by virtue of large resonance effects.

Acknowledgment. This project was supported by National Science Foundation Grant CHE 87-05703. NMR spectroscopy was performed in the University of Iowa High Field NMR Facility.

Registry No. (F8-TPP)FeCl, 99038-25-2; $(F8\text{-}TPP)FeCl^+$, 98715-99-2; $(F8\text{-}TPP)FeCl^{2+}$, 136546-09-3; (F8-TPP)FeF, 124225-64-5; $(F8\text{-}TPP)FeF^+$, 136546-08-2; $(F8\text{-}TPP)FeF^{2+}$, 136546-10-6; $[((pyrr\text{-}d_8)\text{-}F8\text{-}TPP)Fe]_2O$, 136546-11-7; $[((pyrr\text{-}d_8)\text{-}F^*\text{-}TPP)Fe]_2O^+$, 136546-12-8; $[((pyrr\text{-}d_8)\text{-}F8\text{-}TPP)Fe]_2O^{2+}$, 136546-13-9; CH_2Cl_2, 75-09-2; CH_3NO_2, 75-52-5.

(19) Hansen, L. K.; Chang, C. K.; Davis, M. S.; Fajer, J. *J. Am. Chem. Soc.* **1981**, *103*, 663–670.
(20) Dolphin, D.; Felton, R. H. *Acc. Chem. Res.* **1974**, *7*, 26–32.
(21) Spaulding, L. D.; Eller, P. G.; Bertrand, J. A.; Felton, R. H. *J. Am. Chem. Soc.* **1974**, *96*, 982–987.
(22) Fajer, J.; Borg, D. C.; Forman, A.; Adler, A. D.; Varadi, V. *J. Am. Chem. Soc.* **1974**, *96*, 1238–1239.
(23) Boersma, A. D.; Goff, H. M. *Inorg. Chem.* **1984**, *23*, 1671–1676.
(24) Icli, S.; Kreilick, R. W. *J. Phys. Chem.* **1971**, *75*, 3462–3465.